Pericyclic Reactions

DOI: 10.1002/anie.201104465

Electronic Bond-to-Bond Fluxes in Pericyclic Reactions: Synchronous or Asynchronous?**

Timm Bredtmann and Jörn Manz**

Dedicated to Dr. med. Emma Auch-Dorsch

Are new bonds made and old ones broken synchronously or asynchronously during pericyclic reactions, in the electronic ground state? For almost three decades investigations have focused on nuclear rearrangements, first by conjectures based on the energetics of barriers (B) or transition states that separate reactants (R) from products (P), and then by classical molecular dynamics simulations.[1–7] Complementary aspects of the time-independent electronic structures of R, B, and P have also been considered, in the context of the Woodward–Hoffmann rules for the conservation of orbital symmetry[8,9] and analyses of transition structures or intermediates.[10–13]

Herein we address the analogous question of the synchronicity of the electronic fluxes during pericyclic reactions. Specifically, we discover significant differences for reactions with energy E well above the barrier B or well below B. The former scenario ($E > \mathrm{B}$) can be initialized by means of selective laser pulses,[14] whereas the latter ($E < \mathrm{B}$) corresponds to coherent tunneling at cryogenic temperatures.[15] Our investigation is stimulated by the rich phenomena of electronic fluxes[16] and by fundamental experimental and theoretical advances, ranging from femtosecond chemistry for analyses of nuclear dynamics[17] to attosecond chemistry for electron dynamics.[18–20] The underlying methods and models are adapted from Refs. [21–23]. For complementary approaches to electronic fluxes during processes involving two or more electronic states, for example, photochemical reactions, see Refs. [24–28].

As an example, we consider the degenerate [3,3] sigmatropic shift, or the degenerate Cope rearrangement (DCR), of semibullvalene (SBV), in the electronic ground state (see Figure 1). This system and several derivatives have already served as touchstones for various aspects of pericyclic reactivity, from synthesis[11,29,30] to spectroscopy[31,32] and kinetics[31] to electronic structure[11,33–35] and the related thermochromicity[11,30] and laser control.[30] A comprehensive list of references is provided in Ref. [23].

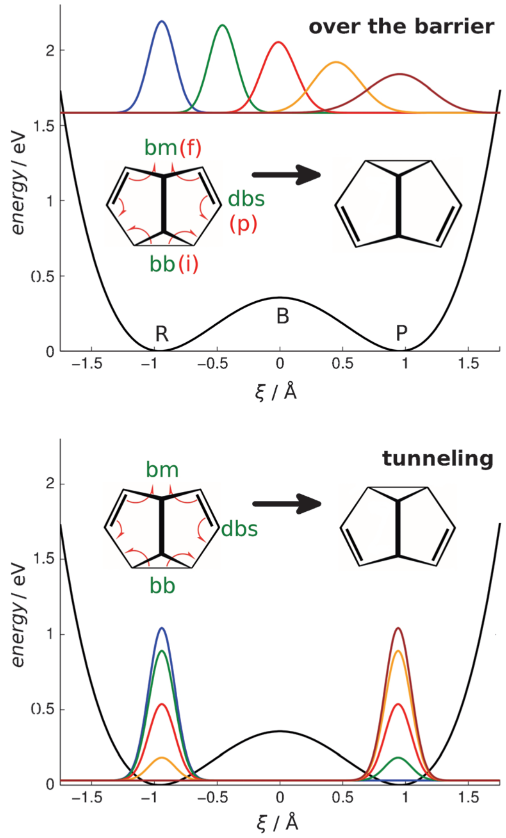

Figure 1. Degenerate Cope rearrangement of semibullvalene for energies E well above the barrier (B) (top) and below B (coherent tunneling, bottom). The Lewis structures of the reactant (R) and product (P) are shown by bird's-eye views. Bond-to-bond fluxes of pericyclic electrons are symbolized by curved arrows. The corresponding bond breaking, bond making, and double-bond shifting are denoted bb, bm, and dbs, respectively. For $E > \mathrm{B}$, the labels i, f, and p denote asynchronous initial, final, and perpetual electronic fluxes, respectively. For $E < \mathrm{B}$, the labels i, p, and f are missing because all electronic fluxes are synchronous. The nuclear wavepacket dynamics is illustrated by five snapshots of the nuclear densities embedded in one-dimensional cuts of the potential energy surface along the path ξ from R via B to P (adapted from Ref. [23]). The snapshots are taken at equidistant times $t_i = (i/4)\,\tau$, $i = 0, 1, 2, 3, 4$, where $\tau = 20.4$ fs and 970 s[15] for $E > \mathrm{B}$ and $E < \mathrm{B}$, respectively. The energies E serve as baselines for the nuclear densities.

The present investigation is based, in particular, on the results of three recent publications:

1) Simulations of the DCR of SBV by Zhang et al. [15] by means of transition-state theory with quantum correc-

---

[*] T. Bredtmann, Prof. Dr. J. Manz
Institut für Chemie und Biochemie, Freie Universität Berlin
Takustrasse 3, 14195 Berlin (Germany)
E-mail: bredt@chemie.fu-berlin.de
jmanz@chemie.fu-berlin.de

[**] We would like to thank Professors W. T. Borden, D. J. Diestler, K. N. Houk, D. A. Hrovat, H. Kono, B. Paulus, H. Quast, K. Takatsuka, W. Thiel, and R. V. Williams for helpful discussions and encouragement, and Prof. H.-C. Hege and F. Marquardt for introducing us to the program Amira for visualization. Financial support by Deutsche Forschungsgemeinschaft (project Ma 515/25-1) and Fonds der Chemischen Industrie is also gratefully acknowledged.

tions.[36] Accordingly, for temperatures below 50 K, the reaction proceeds by coherent tunneling within $\tau = 970$ s.

2) The theory of electronic fluxes in the limit of coherent tunneling ($E < \mathrm{B}$), exemplified for cyclooctatetraene.[22] Here it is applied to SBV using the result $\tau = 970$ s.[15]
3) The theory of electronic bond-to-bond fluxes during the DCR of SBV for $E > \mathrm{B}$, exemplified for the fluxes of "pericyclic" electrons which account for the mutation of the Lewis structure from R to P.[23] We vary energy E to demonstrate the robustness of the results irrespective of the reaction time τ ($\tau = 27.3$ fs for $E = 1.04$ eV in Ref. [23] and $\tau = 20.4$ fs for $E = 1.58$ eV here).

For reference, we first compare the nuclear wavepacket dynamics of the DCR of SBV in the two energy domains (Figure 1). The results confirm traditional knowledge: a) Coherent tunneling is much slower ($\tau = 970$ s[15]) than the reaction above the barrier (here: $\tau = 20.4$ fs). b) For the case of coherent tunneling, the nuclear densities consist essentially of two parts representing R and P. These are superimposed with decreasing and increasing weights or probabilities (P), respectively [Eq. (1)].[22,37,38] They never visit the domain between R and P significantly. In contrast, the reaction over the barrier is represented by a nuclear wavepacket which evolves gradually from R via the domain between R and P to P.

$$P_{\mathrm{R}}(t) = \cos^2(\tfrac{1}{2}\pi t/\tau),\ P_{\mathrm{P}}(t) = \sin^2(\tfrac{1}{2}\pi t/\tau) \qquad (1)$$

For qualitative inspection, the corresponding electronic wavepacket dynamics for the DCR of SBV in the two energy domains are compared in Figure 2. Significant differences are obvious from the snapshots of the electron densities, which are taken at the same times as the nuclear densities shown in Figure 1. Apparently, the different nuclear dynamics for $E < \mathrm{B}$ and $E > \mathrm{B}$ translate into corresponding phenomena of electron dynamics, including the different time scales (a). For item (b), in the domain of coherent tunneling ($E < \mathrm{B}$), the electron density consists essentially of two parts representing R and P, which are superimposed with the same weights as for the nuclear dynamics [Eq. (1)]. In contrast, for $E > \mathrm{B}$, the electron density has lobes that evolve gradually from R to P. Note that different lobes evolve with different speeds. For example, at $t = \tau/4$, the light-gray equidensity contours indicate already the formation of the "new" bond of R for $E < \mathrm{B}$ (tunneling), but not yet for $E > \mathrm{B}$ (over the barrier). At the same time, the dark equidensity contours illustrate the breaking of the "old" bond of R for both cases, $E < \mathrm{B}$ and $E > \mathrm{B}$. This comparison points to qualitative differences of the electronic motions: For $E > \mathrm{B}$ it starts with initial (i) bond breaking (bb), followed by final (f) bond making, accompanied by perpetual (p) double-bond shifting (dbs). In contrast, for $E < \mathrm{B}$, all electronic processes—bm, bb, dbs—proceed synchronously. The differences in the electronic wavepacket dynamics (Figure 2) correspond to the differences in the nuclear wavepacket dynamics (Figure 1).

The qualitative conclusions drawn from Figure 2 are quantified by the results for the electronic fluxes during the DCR of SBV with energies $E > \mathrm{B}$ and $E < \mathrm{B}$ as shown in the left and right top panels of Figure 3, respectively. As anticipated in the discussion of Figure 2, for $E > \mathrm{B}$, the electrons initially (i) flow out of the breaking bond before they finally (f) enter the new bond, that is, asynchronicity. At the same time, there are rather weak "perpetual" (p) electronic fluxes which account for dbs. The corresponding time-integrated "initial" and "final" electronic fluxes form a hysteresis (cf. the left panels in Figure 3). In contrast, in the limit of coherent tunneling ($E < \mathrm{B}$), fluxes and time-inte-

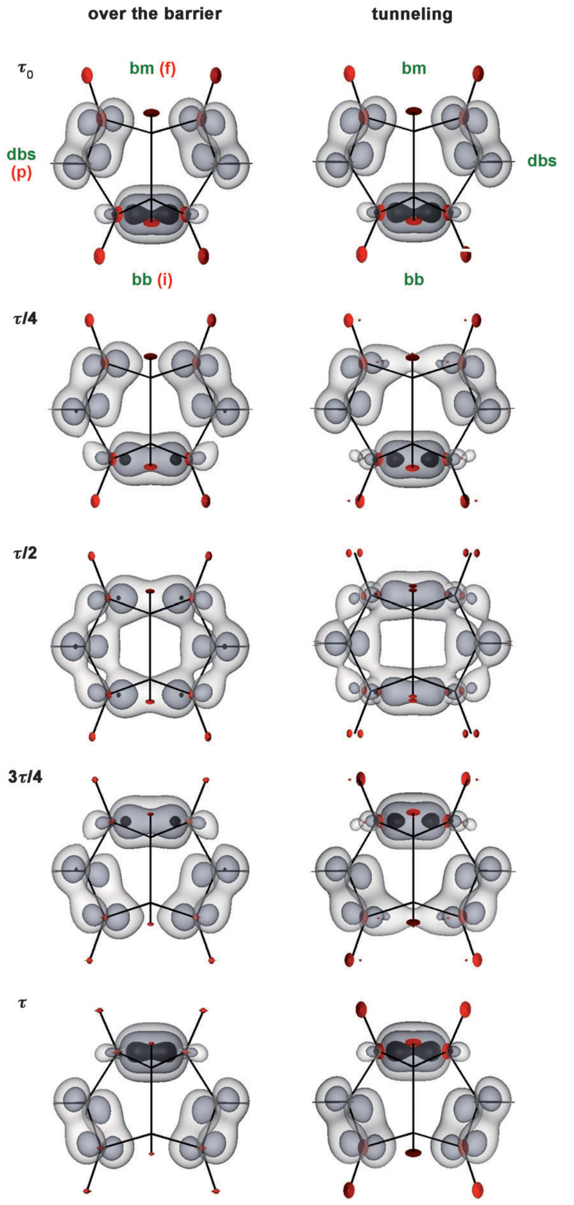

Figure 2. Comparison of the time evolutions of pericyclic electrons during the degenerate Cope rearrangement of semibullvalene with energies E above (left) and below (right) the barrier B, shown as three nested equidensity contours with values: 0.236 Å^{-3} (light gray), 0.506 Å^{-3} (gray), and 1.114 Å^{-3} (dark). The acronyms are the same as in Figure 1. The nuclear wavepacket dynamics is illustrated in red. The snapshots correspond to the same times as shown in Figure 1. The program Amira[39,40] was used for data visualization.

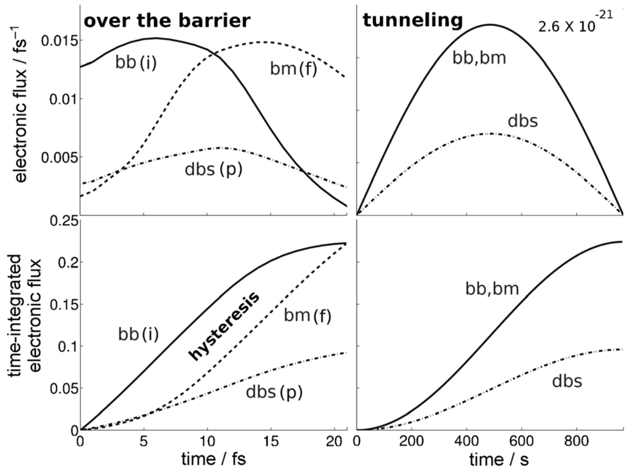

Figure 3. Comparison of the asynchronous (left) versus synchronous (right) electronic fluxes (top panels) and the time-integrated fluxes (bottom panels) during the degenerate Cope rearrangement of semibullvalene with energies *E* above and below the barrier B, respectively. The acronyms are the same as in Figure 1.

grated fluxes all evolve according to the same law,[22] Equation (1). The hysteresis thus collapses to a single line, owing to the underlying synchronicity of the electronic fluxes for bb and bm (cf. the right panels in Figure 3).

In conclusion, electronic fluxes during a given pericyclic reaction in the electronic ground state may proceed either synchronously or asynchronously. The mechanism is determined by the preparation of the reactants, for example, synchronous at cryogenic temperatures ($E < \mathrm{B}$) but asynchronous when induced by selective laser pulses ($E > \mathrm{B}$). In extrapolation to reactions under ambient conditions, the value of $k_\mathrm{B}T$ matters; in the present case, without laser excitation, the relation $k_\mathrm{B}T < \mathrm{B}$ suggests a dominant contribution of tunneling. The electronic fluxes for bb and bm should, therefore, be preferably synchronous at room temperature, similar to the result for $E < \mathrm{B}$. The present example should stimulate systematic experimental[18,19] and theoretical investigations of these phenomena in pericyclic reactions.

Received: June 28, 2011
Published online: November 4, 2011

Keywords: electronic fluxes · pericyclic reactions · quantum dynamics · reaction mechanisms · synchronicity

---

[1] M. J. S. Dewar, *J. Am. Chem. Soc.* **1984**, *106*, 209.
[2] W. T. Borden, R. J. Loncharich, K. N. Houk, *Annu. Rev. Phys. Chem.* **1988**, *39*, 213.
[3] K. N. Houk, Y. Li, J. D. Evanseck, *Angew. Chem.* **1992**, *104*, 711; *Angew. Chem. Int. Ed. Engl.* **1992**, *31*, 682.
[4] R. A. Marcus, *J. Am. Chem. Soc.* **1995**, *117*, 4683.
[5] H. Ushiyama, K. Takatsuka, *J. Chem. Phys.* **2001**, *115*, 5903.
[6] T. Rozgonyi, A. Bartók-Pártay, A. Stirling, *J. Phys. Chem. A* **2010**, *114*, 1207.
[7] L. Xu, C. E. Doubleday, K. N. Houk, *J. Am. Chem. Soc.* **2010**, *132*, 3029.
[8] R. B. Woodward, R. Hoffmann, *The Conservation of Orbital Symmetry*, Verlag Chemie, Weinheim, **1970**.
[9] I. Fleming. *Pericyclic Reactions*, Oxford University Press, **1998**.
[10] V. N. Staroverov, E. R. Davidson, *J. Am. Chem. Soc.* **2000**, *122*, 7377.
[11] R. V. Williams, *Chem. Rev.* **2001**, *101*, 1185.
[12] H. Lischka, E. Ventura, M. Dallos, *ChemPhysChem* **2004**, *5*, 1365.
[13] P. R. Griffiths, D. E. Pivonka, R. V. Williams, *Chem. Eur. J.* **2011**, *17*, 9193.
[14] I. Iwakura, A. Yabushita, T. Kobayashi, *Chem. Lett.* **2010**, *39*, 374.
[15] X. Zhang, D. A. Hrovat, W. T. Borden, *Org. Lett.* **2010**, *12*, 2798.
[16] *Current-Driven Phenomena in Nanoelectronics* (Ed.: T. Seideman), Pan Stanford Publishing, Singapore, **2011**.
[17] A. H. Zewail, *Angew. Chem.* **2000**, *112*, 2688; *Angew. Chem. Int. Ed.* **2000**, *39*, 2586.
[18] F. Krausz, M. Ivanov, *Rev. Mod. Phys.* **2009**, *81*, 163.
[19] *Quantum Dynamic Imaging* (Eds.: A. D. Bandrauk, M. Y. Ivanov), Springer, New York, **2011**.
[20] T. Bredtmann, S. Chelkowski, A. D. Bandrauk, *Phys. Rev. A* **2011**, *84*, 021401(R).
[21] I. Barth, H.-C. Hege, H. Ikeda, A. Kenfack, M. Koppitz, J. Manz, F. Marquardt, G. K. Paramonov, *Chem. Phys. Lett.* **2009**, *481*, 118.
[22] H.-C. Hege, J. Manz, F. Marquardt, B. Paulus, A. Schild, *Chem. Phys.* **2010**, *376*, 46.
[23] D. Andrae, I. Barth, T. Bredtmann, H.-C. Hege, J. Manz, F. Marquardt, B. Paulus, *J. Phys. Chem. B* **2011**, *115*, 5476.
[24] I. Barth, J. Manz, *Angew. Chem.* **2006**, *118*, 3028; *Angew. Chem. Int. Ed.* **2006**, *45*, 2962.
[25] I. Barth, J. Manz, Y. Shigeta, K. Yagi, *J. Am. Chem. Soc.* **2006**, *128*, 7043.
[26] M. Kanno, H. Kono, Y. Fujimura, *Angew. Chem.* **2006**, *118*, 8163; *Angew. Chem. Int. Ed.* **2006**, *45*, 7995.
[27] M. Okuyama, K. Takatsuka, *Chem. Phys. Lett.* **2009**, *476*, 109.
[28] K. Nagashima, K. Takatsuka, *J. Phys. Chem. A* **2009**, *113*, 15240.
[29] H. E. Zimmerman, G. L. Grunewald, *J. Am. Chem. Soc.* **1966**, *88*, 183.
[30] M. Dohle, J. Manz, G. K. Paramonov, H. Quast, *Chem. Phys.* **1995**, *197*, 91.
[31] A. K. Cheng, F. A. L. Anet, J. Mioduski, J. Meinwald, *J. Am. Chem. Soc.* **1974**, *96*, 2887.
[32] M. Seefelder, M. Heubes, H. Quast, W. D. Edwards, J. R. Armaentrout, R. V. Williams, C. J. Cramer, A. C. Goren, D. A. Hrovat, W. T. Borden, *J. Org. Chem.* **2005**, *70*, 3437.
[33] M. Garavelli, F. Bernardi, A. Cembran, O. Castaño, L. M. Frutos, M. Merchán, M. Olivucci, *J. Am. Chem. Soc.* **2002**, *124*, 13770.
[34] H. Jiao, R. Nagelkerke, H. A. Kurtz, R. V. Williams, W. T. Borden, P. von R. Schleyer, *J. Am. Chem. Soc.* **1997**, *119*, 5921.
[35] E. C. Brown, D. K. Henze, W. T. Borden, *J. Am. Chem. Soc.* **2002**, *124*, 14977.
[36] A. Fernandez-Ramos, B. A. Ellingson, B. C. Garrett, D. G. Truhlar, *Reviews in Computational Chemistry, Vol. 23*, Wiley-VCH, Hoboken, NJ, **2007**, pp. 125–232.
[37] J. Brickmann, H. Zimmermann, *Z. Naturforsch. A* **1968**, *23*, 11.
[38] C. Cohen-Tannoudji, B. Diu, F. Laloë, *Quantum Mechanics*, Wiley, New York, **1977**.
[39] D. Stalling, M. Westerhoff, H.-C. Hege, *The Visualization Handbook*, Elsevier, Amsterdam, **2005**.
[40] "Visual analysis of quantum physics data": H.-C. Hege, M. Koppitz, F. Marquardt, C. McDonald, C. Mielack in *Quantum Dynamic Imaging* (Eds.: A. D. Bandrauk, M. Y. Ivanov), Springer, New York, **2011**, pp. 71–87.